Search for the Standard Model Higgs boson and its coupling to fermions with the ATLAS detector

Claire A. Lee
University of Johannesburg, South Africa
E-mail: claire.lee@cern.ch

Abstract. The Higgs boson discovered in 2012 by the ATLAS and CMS experiments at the LHC has been shown to couple to bosons through it's discovery channels. The emphasis since the discovery has since shifted to measurements of its properties. The direct observation of the coupling of the new boson to fermions is of particular importance for determination whether it is indeed the Higgs boson predicted by the Standard Model. A review of the search for the Higgs boson through its decay into b-quark and muon pairs is given.

1. Introduction

The discovery of a particle with a mass of 125.5 GeV by the ATLAS [1] and CMS [2] experiments in 2012 is one of the great successes of the Large Hadron Collider program (LHC) at CERN. The observation was made through the bosonic decay channels $H \to \gamma\gamma$, $H \to ZZ$ and $H \to WW$, indicating that the new particle was itself a boson. Subsequent measurements of its properties focused on the bosonic decay modes due to the better resolution in those channels, but an important question remained: whether or not the new particle also coupled to fermions.

The non-zero vacuum expectation value of the Higgs field spontaneously breaks the electroweak symmetry of the Standard Model (SM), imparting mass on the weak vector bosons and generating a massive scalar boson in the process. The single Higgs field predicted within the framework of the SM also bestows mass on the fermions through their Yukawa coupling, with a strength proportional to their masses. Evidence of these couplings and measurement of their strengths is therefore necessary for determining whether the newly-discovered particle is indeed the SM Higgs boson.

The dominant Higgs production mechanism at the LHC is gluon-gluon fusion (ggF), a process that proceeds through a top quark loop and is therefore an indirect probe of the coupling of the Higgs to the top quark. Additional production mechanisms are vector boson fusion (VBF) which has a signature of two well-separated jets; associated production with a vector boson (VH)[1] where one can trigger on the resulting signature from the V decay; and associated production with a pair of top quarks ($t\bar{t}$H) whose decays give b-tagged jets, leptons and missing transverse momentum in the detector. Values of the cross sections for a 125 GeV Higgs boson at 7 and 8 TeV centre of mass energy are shown in table 1 below:

[1] also called Higgs-strahlung

Process	$\sigma_{7\ \mathrm{TeV}}$ (pb)	$\sigma_{8\ \mathrm{TeV}}$ (pb)
ggF	15.13	19.27
VBF	1.22	1.58
WH	0.58	0.70
ZH	0.34	0.42
$t\bar{t}$H	0.09	0.13

Table 1: Production cross sections for 125 GeV Higgs boson at 7 and 8 TeV centre of mass energy at the LHC.

The final production mechanism, $t\bar{t}$H, allows us to directly probe the top Yukawa coupling via the various decay channels, though it has the smallest production cross section. Coupling of the Higgs to the down-type fermions, however, requires direct observation of their decays, though these channels are particularly challenging at hadron colliders, and require very high performance reconstruction of objects (electrons, muons, tau leptons, jets and the missing transverse energy). The ATLAS experiment has performed searches in the $H \to \tau\tau$ [3], $H \to b\bar{b}$ [4, 5], and $H \to \mu\mu$ [6] fermionic decay channels. The $H \to \tau\tau$ channel is covered in detail by K. Bristow in this same conference, and an overview of the $H \to b\bar{b}$ and $H \to \mu\mu$ analyses is given here.

2. The ATLAS Detector

The ATLAS detector [7] is a multipurpose system of particle detectors with a forward-backward symmetric cylindrical geometry and near 4π solid angle coverage. It is composed of 3 core systems arranged in a barel-plus-endcaps format[2]. The inner detector (ID), covering the pseudorapidity range $|\eta| < 2.5$[3], consists of a silicon pixel detector, a silicon microstrip detector (SCT) and a transition radiation tracker (TRT) within the $|\eta| < 2$ range. The ID is surrounded by a thin superconducting solenoid providing a 2 T magnetic field. A high granularity lead/liquid argon (LAr) sampling electromagnetic calorimeter covers the region $|\eta| < 3.2$ while a steel/scintillator-tile calorimeter provides hadronic coverage within $|\eta| < 1.7$. A Copper-LAr hadronic calorimeter is used in the end-cap region $1.5 < |\eta| < 3.2$. In the forward region, $3.1 < |\eta| < 4.9$, a copper-LAr electromagnetic calorimeter and a copper/tungsten-LAr hadronic calorimeter for a full energy measurement. Finally, the muon spectrometer (MS) surrounds the calorimeters, consisting of three large air-core superconducting toroid magnets, precision tracking chambers providing accurate muon momentum measurement out to $|\eta| < 2.7$, and additional detectors for muon triggers in the region $|\eta| < 2.4$.

3. Search for $VH \to b\bar{b}$

At 57.7%, $H \to b\bar{b}$ has the highest branching ratio of all Higgs decays for a 125 GeV Higgs boson, but only associated production channels are possible at hadron colliders due to the large multijet background. At ATLAS we focus on the VH and $t\bar{t}$H channels separately; here we discuss the $VH \to b\bar{b}$ results, with the $t\bar{t}H \to b\bar{b}$ results in section 4.

The $VH \to b\bar{b}$ analysis covers both 2011 and 2012 LHC data, with 4.7 fb^{-1} at 7 TeV and 20.3 fb^{-1} at 8 TeV. The analysis follows a cut-based approach, with a profile likelihood fit to the m_{bb}

[2] The barrel-region detectors are arranged in concentric cylinders parallel to the beam axis, while the endcap detectors are disks oriented perpendicular to the beam axis.

[3] In ATLAS, the positive x-axis is defined as pointing from the interaction point to the center of the LHC ring, the positive y-axis is defined as pointing upwards, and the positive z-axis corresponds to protons running anticlockwise. The polar angle θ is measured from the beam axis (z-axis), the azimuthal angle ϕ is measured in the transverse (xy)-plane, and the pseudorapidity is defined by $\eta = -\log(\tan(\theta/2))$.

invariant mass, and events are categorised by the number of high p_{T} isolated leptons into the 0,1, or 2 lepton channel, depending on the vector boson decay channel ($Z \to \nu\nu$, W $\to \ell\nu$, and Z $\to \ell\ell$ respectively). All selected events for the analysis require exactly two b-tagged jets, with a p_{T} of 45 (20) GeV for the leading (sub-leading) jet. At most there may be one extra jet in the event.

In the 0 lepton channel, no leptons passing the "loose" identification criteria are allowed, with the $E_{\mathrm{T}}^{\mathrm{miss}}$> 120 GeV, track-based $p_{\mathrm{T}}^{\mathrm{miss}}$> 30 GeV, and a directional requirement matching the $E_{\mathrm{T}}^{\mathrm{miss}}$ and $p_{\mathrm{T}}^{\mathrm{miss}}$.[4] For the 1 lepton channel, the lepton is required to pass the "tight" identification criteria, a $E_{\mathrm{T}}^{\mathrm{miss}}$> 25 GeV cut is applied, and the transverse mass of the W boson is required to be between 40 and 120 GeV. In the 2 lepton case we require 1 medium and 1 loose leptons of same flavour but opposite sign, a dilepton invariant mass within 18 GeVof the Z boson mass, and $E_{\mathrm{T}}^{\mathrm{miss}}$< 60 GeV. Control regions are defined as events with only one b-tagged jet, or events with two different-flavour leptons (top control region).

Events are sub-categorised in bins of vector boson p_{T} and jet multiplicity, with topological requirements to reduce the backgrounds in the different bins individually and thus increase overall sensitivity. A global fit is performed on the $b\bar{b}$ invariant mass distributions in the signal regions and the event yields in the different control regions. Systematics contributing to the overall uncertainties originate from $t\bar{t}$ background modelling uncertainties, the two to three jet ratio, vector boson p_{T}, c-jet tagging efficiencies, multijet normalisations and signal acceptance, and amount to about 3% on the background and 12% on the signal after the fit. A separate diboson fit using the same configuration as the Higgs signal is performed to extract the signal strength parameter μ_{VZ} from $VZ \to b\bar{b}$ decay and validate the analysis method, with a result of $\mu_{VZ} = 0.9 \pm 0.2$, consistent with the SM.

Figure 1 shows the 95% CL upper limits [8, 9, 10] on the Higgs boson production cross section in the range 110 - 150 GeV for this channel. No significant excess is observed, with a best-fit signal strength of $\mu = 0.2 \pm 0.5(\mathrm{stat.}) \pm 0.4(\mathrm{syst.})$. The observed (expected) 95% CL upper limit on the $VH \to b\bar{b}$ signal strength for a 125 GeV Higgs boson is set as 1.4 (1.3) times the SM production cross section.

4. Search for $t\bar{t}H \to b\bar{b}$

In the $t\bar{t}H \to b\bar{b}$ channel, a multivariate analysis on 20.3 fb^{-1} of 8 TeV LHC data is performed to discriminate the signal from the overwhelming $t\bar{t}$+ jets background. Events are categorised by number of high p_{T} leptons (1 or 2), allowing for events where one of the W bosons decays either hadronically or leptonically (the other W boson is always required to decay leptonically). The events are further classified depending on their jet and b-tagged jet multiplicities; In the single lepton channel nine independent regions are considered, requiring at least 4 jets where at least 2 of which are b-tagged, while six independent regions cover the dilepton channel, where at least 2 jets with at least 2 b-tags are required.

Events are selected that contain either 1 or 2 leptons with p_{T} greater than 25 GeV (or 15 GeV for the sub-leading lepton in the dilepton channel). Additionally, in the dilepton channel further cuts are applied to suppress contributions from resonances such as the J/ψ, Υ and Z that decay to lepton pairs. No requirement on the $E_{\mathrm{T}}^{\mathrm{miss}}$ is made, since after all the selections

[4] The track-based transverse missing momentum, $p_{\mathrm{T}}^{\mathrm{miss}}$, is the transverse momentum calculated solely from tracks in the ATLAS Inner Detector originating from the hard scatter vertex. It is almost completely decoupled from the calorimetric $E_{\mathrm{T}}^{\mathrm{miss}}$ measurement and independent of the effects of pileup, making it a good complement to the $E_{\mathrm{T}}^{\mathrm{miss}}$measurement and a useful tool for rejecting events with fake $E_{\mathrm{T}}^{\mathrm{miss}}$.

the sample is dominated by $t\bar{t}$+ jets in both channels.

Signal-rich regions, depending on their jet multiplicities, are defined according to their $S/\sqrt{B}$ ratio, combining events with both e and μ flavours of leptons. The signal-rich regions are the (5j, ≥4b), (≥6j, 3b) and (≥6j, ≥4b) regions for single lepton events, and (≥4j, 3b) and (≥4j, ≥4b) regions for dilepton events.[5] In these regions, a neural network (NN) is used to discriminate signal from background, while in the other, signal-depleted regions, the scalar sum of the jet p_{T} H_T^{had} (jet and lepton p_{T} H_T in the dilepton channel) is used due to the lower sensitivity. The NNs are built using the NeuroBayes package [11], with 10 variables entering the discriminant to give a close-to-optimal signal-to-background separation. The variables used cover object kinematics, global event variables, event shape and object pair properties, and those used in one region are required to be well described by Monte Carlo simulations in other regions too.

A simultaneous binned likelihood fit to the discriminants of each of the analysis regions (NN output in the signal-rich regions, and $H_T^{(had)}$ in the signal-depleted regions) is performed under the signal-plus-background hypothesis, to extract the signal strength parameter μ (which is allowed to float freely in the fit but required to be equal in all fit regions). Dominant systematics are due to the normalisation of the $t\bar{t}$ + heavy flavour background, flavour tagging efficiencies, $t\bar{t}$ reweighting and the jet energy scale, and amount to around 7% on the signal and 20% on the background after the fit.

The fitted signal strength for a 125 GeV Higgs boson in the $t\bar{t}H \to b\bar{b}$ channel is found to be $\mu = 1.7 \pm 1.4$, and a signal 4.1 times larger than predicted by the SM is excluded at 95% CL (the expected exclusion limit is 2.6 larger). The post-fit event yields per bin ordered by $\log(S/B)$ are shown for all bins and both channels combined in figure 2, where the signal is normalised to the best-fit value of μ.

5. Search for $H \to \mu\mu$

Finally, a search spanning the ggF, VH and VBF production mechanisms is conducted on 24.8 fb^{-1} of 7 and 8 TeV data in the $\mu\mu$ decay channel, the only channel currently available for measuring the Higgs coupling to second generation fermions. This channel provides a clean final state, but suffers from a very small branching ratio (0.0219%) and large SM backgrounds. Exactly two muons are selected in the final state, with p_{T}> 25 (15) GeV for the leading (subleading) muon, and events are required to have $E_{\mathrm{T}}^{\mathrm{miss}} < 80$ GeV to suppress $t\bar{t}$ and diboson backgrounds.

To maximise sensitivity to the Higgs signal, 7 mutually exclusive categories are defined. Events with two forward jets with an invariant mass greater than 500 GeV, $|\eta_{jet1} - \eta_{jet2}| > 3$, and $\eta_{jet1} \times \eta_{jet2} < 0$ are selected for the VBF category, based on the resulting dijet signature from the VBF production (events with jets identified as originating from a b-quark are vetoed). The events that are not selected for the VBF category are then classified using $p_{\mathrm{T}}{}^{\mu\mu}$ into low ($p_{\mathrm{T}\mu\mu} < 15$ GeV), medium ($15 < p_{\mathrm{T}\mu\mu} <$50 GeV) and high ($p_{\mathrm{T}\mu\mu} > 50$ GeV) regions. Each category is then further divided into two categories - central and non-central (based on the $|\eta|$ distributions of the two selected muons) - to exploit the more precise muon p_{T} measurement in the central region.

A binned maximum likelihood fit is simultaneously performed on the $m_{\mu\mu}$ distribution in

[5] (xj, yb) implies events with x jets, of which y are b-tagged.

each category, though separate distributions are used for the 7 and 8 TeV data samples. The background PDF for the $p_{\mathrm{T}\mu\mu}$ categories is defined as the sum of a Breit-Wigner (BW) function convolved with a Gaussian, and an exponential function divided by $(m_{\mu_1\mu_2})^3$. For the VBF category, the product of a BW and an exponential function is used. For all categories, the mean and width of the BW peak are fixed to the world average values for those of the Z boson, of $m_{BW} = 91.2$ GeV and $\Gamma_{BW} = 2.49$ GeV. The signal PDF is obtained from Higgs MC samples with ggF, VBF and VH processes combined, and is parametrised as a sum of a Crystal Ball and Gaussian PDF.

Main systematic uncertainties for the number of expected signal events include the uncertainty on the $H \to \mu\mu$ branching ratio ($\pm 7\%$), QCD scale and PDF predictions (± 8 % each for ggF) and the ggF uncertainty in VBF (± 22 %). Experimentally, the dominant sources of uncertainty come from the luminosity estimation, of $\pm 1.8\%$ for 7 TeV data, and $\pm 2.8\%$ for 7 TeV data, and the jet energy scale $\sim 4.5\%$ (VBF).

The invariant dimuon mass spectrum $m_{\mu\mu}$ is shown in figure 3 for both 7 and 8 TeV data combined. No evidence for a narrow peak in the $m_{\mu\mu}$ distribution is observed. A 95% CL upper limit on the signal strength for a 125.5 GeV Higgs boson is set at 7.0 times the SM prediction, where 7.2 is expected. Assuming a Higgs boson mass of 125.2 GeV and the SM production cross section, the 95% CL upper limit on the $H \to \mu\mu$ branching ratio is set at 1.5×10^{-3}

6. Conclusions

A search for the Standard Model Higgs boson of mass 125 GeV through its fermionic decay channels has been performed using 7 and 8 TeV data from Run 1 at the LHC. In the $VH \to b\bar{b}$, $t\bar{t}H \to b\bar{b}$ and $H \to \mu\mu$ channels, no significant excesses were observed over the background, with observed (expected) limits of 1.4 (1.3), 4.1 (2.6) and 7.0 (7.2) $\times$ SM respectively. Overall, the results show no significant deviations from the Standard Model, and we look forward to final updated results on the Run 1 analyses and to the higher energy regime that will be probed during the LHC Run 2.

References

[1] ATLAS Collaboration, *Observation of a new particle in the search for the Standard Model Higgs boson with the ATLAS detector at the LHC*, Phys. Lett. B 716 (2012) 1, arXiv:1207.7214 [hep-ex].

[2] CMS Collaboration, *Observation of a new boson at a mass of 125 GeV with the CMS experiment at the LHC*, Phys. Lett. B 716 (2012) 30, arXiv:1207.7235 [hep-ex].

[3] ATLAS Collaboration, *Evidence for Higgs Boson Decays to the $\tau^+\tau^-$ Final State with the ATLAS Detector*, ATLAS-CONF-2013-108.

[4] ATLAS Collaboration, *Search for the $b\bar{b}$ decay of the Standard Model Higgs boson in associated $(W/Z)H$ production with the ATLAS detector*, ATLAS-CONF-2013-079.

[5] ATLAS Collaboration, *Search for the Standard Model Higgs boson produced in association with top quarks decaying into $b\bar{b}$ in pp collisions at $\sqrt{s}$ = 8 TeV with the ATLAS detector at the LHC*, ATLAS-CONF-2014-011.

[6] ATLAS Collaboration, *Search for the Standard Model Higgs boson decay to $\mu + \mu^-$ with the ATLAS detector*, arXiv:1406.7663v1 [hep-ex].

[7] ATLAS Collaboration, *The ATLAS Experiment at the CERN Large Hadron Collider*, JINST 3 (2008) S08003.

[8] T. Junk, *Condence level computation for combining searches with small statistics*, Nucl. Instr. Meth. A 434 (1999) 435, arXiv:9902006 [hep-ex].

[9] A. L. Read, *Presentation of search results: the CLs technique*, J. Phys. G 28 (2002) 2693.

[10] G. Cowan, K. Cranmer, E. Gross, and O. Vitells, *Asymptotic formulae for likelihood-based tests of new physics*, Eur. Phys. J. C 71 (2011) 1554, arXiv:1007.1727 [physics.data-an].

[11] Phi-T GmbH, *NeuroBayes package*, http://neurobayes.phi-t.de/

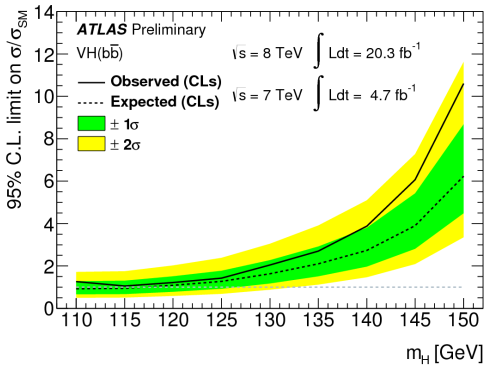

Figure 1: 95% CL upper limits on the Higgs boson production cross section in the range 110 - 150 GeVfor the $VH \to b\bar{b}$ channel.

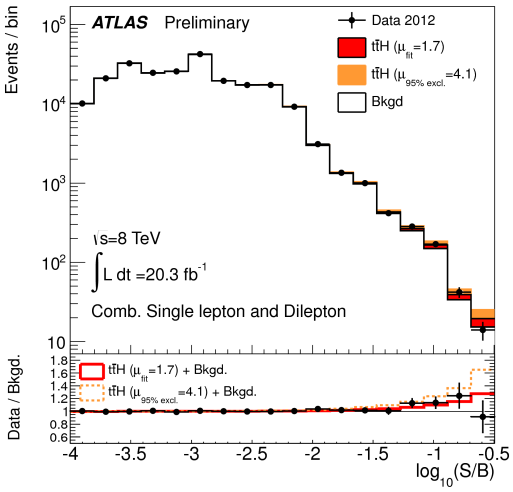

Figure 2: Post-fit $t\bar{t}H \to b\bar{b}$ event yields per bin ordered by $\log(S/B)$ for all bins and both channels combined. The signal is normalised to the best-fit value of μ.

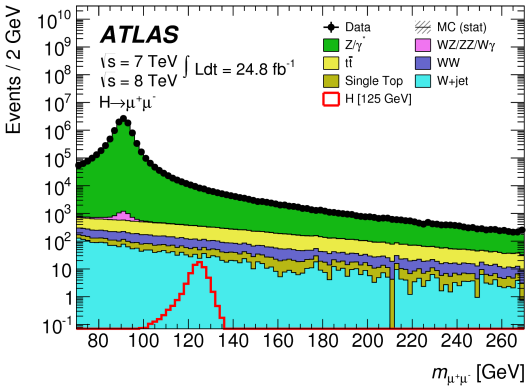

Figure 3: Invariant dimuon mass spectrum $m_{\mu\mu}$ for 7 and 8 TeV data combined.